Solar Mg appendix

Sun · Mg · downloadable appendix

Document	Solar Mg appendix
Subject	Solar photospheric abundance appendix · Mg
Author	Ryan Schmitt
Date	2026-10-28
Publisher	The Exoplanet Codex · exoplanetcodex.org
Version	feed v1.336
Source	science commit a1130fc6ecc7
Web	https://exoplanetcodex.org/systems/sol/elements/mg/

Solar magnesium: 7.668 ± 0.043

Asplund, Amarsi & Grevesse 2021: 7.55 ± 0.03 · this measurement +0.118 dex

The three-dimensional non-LTE products apply published line-by-line corrections (Asplund et al. 2021) to our one-dimensional fits; they are not our own three-dimensional calculation. The K-band products are the first for magnesium. No second telluric correction exists in the K band, so their telluric error is scaled from the J band of the same night.

Combined the way Asplund, Amarsi & Grevesse (2021) combine it: weighted mean and error of the indicator families Mg I, Mg II (Asplund+2021 Sect. 2.4); inverse total-variance weights; statistical parts combined as independent, systematic parts as shared (Amarsi+2021 Eq. 3). Each indicator is represented by our best analysis of it.

Mg I: 7.661 ± 0.041 · IAG FTS · red-optical · Mg I · Asplund et al. 2021 lines · 3D NLTE (Amarsi)

Mg II: 7.717 ± 0.106 · Kitt Peak (1984, molecfit) · NIR · Mg II · Asplund et al. 2021 lines · 3D NLTE (Amarsi)

Highlighted Products

VIS

7.646 ± 0.036

Mg I · Asplund et al. 2021 lines · 3D NLTE (Amarsi) · HARPS · Reference Grade

red-optical

7.661 ± 0.041

Mg I · Asplund et al. 2021 lines · 3D NLTE (Amarsi) · IAG FTS · Reference Grade

NIR

7.717 ± 0.106

Mg II · Asplund et al. 2021 lines · 3D NLTE (Amarsi) · Kitt Peak (1984, molecfit) · Reference Grade

H

7.568 ± 0.055

Mg I · Asplund et al. 2021 lines · 3D NLTE (Amarsi) · CRIRES+ H (full arm, telluric-corrected) · Reference Grade

K

7.507 ± 0.060

Mg I · Codex-graded lines · 1D NLTE (Gerber) · CRIRES+ · Codex Grade

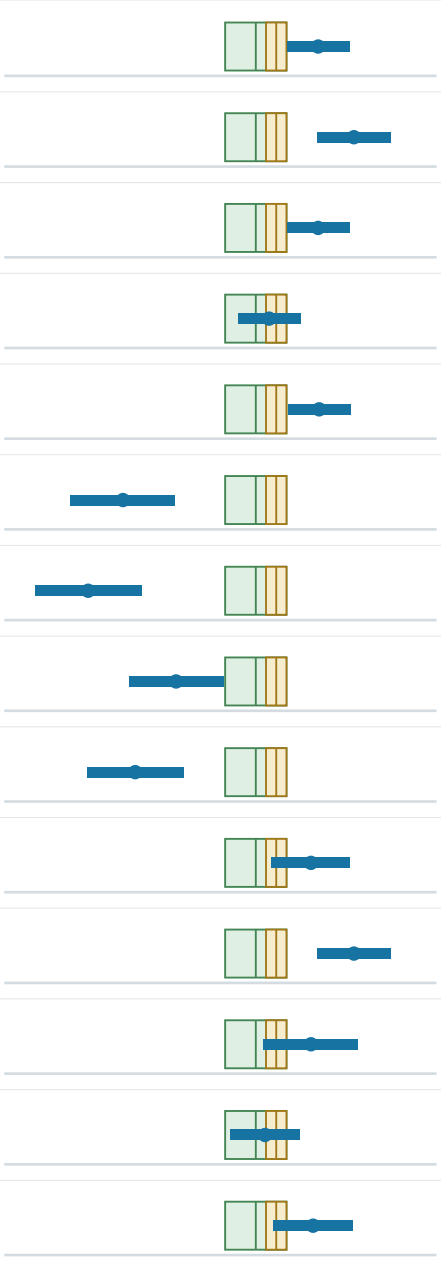
Line grades

Every product is measured on one of three grades of spectral lines and the grades are never mixed in one number.

Grade	What it means	This element
Reference Grade	lines from a published solar line set (Asplund et al. 2021 and similar), measured with the oscillator strengths the authors used	98 products -- Mg I · Asplund et al. 2021 lines; Mg II · Asplund et al. 2021 lines; SET-MG_BERGEMANN2017
Codex Grade	lines chosen by the Codex whose oscillator strength carries a published uncertainty (laboratory measurement, NIST accuracy class A-C, or the paper's own stated error), between 5% and 60% deep	83 products -- Mg I · Codex-graded lines; Mg II · Codex-graded lines
Deep Grade	the same oscillator-strength rule on lines deeper than 60% -- stronger lines, more sensitive to damping and the model atmosphere	12 products -- Mg I · Deep-graded lines

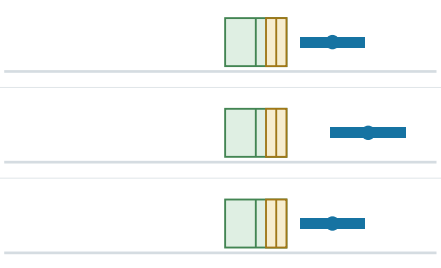
Error-bar Forest Plot

VIS — HARPS
A(Mg) dex; axis 7.30–7.73



Mg I · Asplund et al. 2021 lines · 1D LTE Reference Grade · 2 lines	7.611 ±0.031
Mg I · Asplund et al. 2021 lines · 3D NLTE (Amarsi) Reference Grade · 2 lines	7.646 ±0.036
Mg I · Asplund et al. 2021 lines · 1D NLTE (Amarsi) Reference Grade · 2 lines	7.611 ±0.031
Mg I · Asplund et al. 2021 lines · 1D NLTE (Gerber) Reference Grade · 2 lines	7.563 ±0.030
Mg I · Asplund et al. 2021 lines · 1D LTE (Gerber) Reference Grade · 2 lines	7.612 ±0.031
Mg I · Deep-graded lines · 1D LTE Deep Grade · 6 lines	7.420 ±0.051
Mg I · Deep-graded lines · 1D NLTE (Amarsi) Deep Grade · 4 lines	7.386 ±0.052
Mg I · Deep-graded lines · 1D NLTE (Gerber) Deep Grade · 6 lines	7.472 ±0.046
Mg I · Deep-graded lines · 1D LTE (Gerber) Deep Grade · 6 lines	7.432 ±0.047
Mg I · Codex-graded lines · 1D LTE Codex Grade · 3 lines	7.604 ±0.038
Mg I · Codex-graded lines · 3D NLTE (Amarsi) Codex Grade · 2 lines	7.646 ±0.036
Mg I · Codex-graded lines · 1D NLTE (Amarsi) Codex Grade · 3 lines	7.604 ±0.046
Mg I · Codex-graded lines · 1D NLTE (Gerber) Codex Grade · 3 lines	7.559 ±0.034
Mg I · Codex-graded lines · 1D LTE (Gerber) Codex Grade · 3 lines	7.606 ±0.039

VIS — Kitt Peak (Kurucz 2005)
A(Mg) dex; axis 7.30–7.73



Mg I · Asplund et al. 2021 lines · 1D LTE Reference Grade · 2 lines	7.625 ±0.032
Mg I · Asplund et al. 2021 lines · 3D NLTE (Amarsi) Reference Grade · 2 lines	7.660 ±0.037
Mg I · Asplund et al. 2021 lines · 1D NLTE (Amarsi) Reference Grade · 2 lines	7.625 ±0.032

VIS — Kitt Peak (Kurucz 2005)
A(Mg) dex; axis 7.30–7.73

Mg I · Asplund et al. 2021 lines · 1D NLTE (Gerber) Reference Grade · 2 lines		7.612 ±0.030
Mg I · Asplund et al. 2021 lines · 1D LTE (Gerber) Reference Grade · 2 lines		7.627 ±0.032
Mg I · Deep-graded lines · 1D LTE Deep Grade · 6 lines		7.390 ±0.046
Mg I · Deep-graded lines · 1D NLTE (Amarsi) Deep Grade · 4 lines		7.384 ±0.049
Mg I · Deep-graded lines · 1D NLTE (Gerber) Deep Grade · 6 lines		7.414 ±0.049
Mg I · Deep-graded lines · 1D LTE (Gerber) Deep Grade · 6 lines		7.414 ±0.044
Mg I · Codex-graded lines · 1D LTE Codex Grade · 3 lines		7.615 ±0.058
Mg I · Codex-graded lines · 3D NLTE (Amarsi) Codex Grade · 2 lines		7.660 ±0.037
Mg I · Codex-graded lines · 1D NLTE (Amarsi) Codex Grade · 3 lines		7.615 ±0.068
Mg I · Codex-graded lines · 1D NLTE (Gerber) Codex Grade · 3 lines		7.607 ±0.060
Mg I · Codex-graded lines · 1D LTE (Gerber) Codex Grade · 3 lines		7.617 ±0.058

VIS — Kitt Peak (1984, molecfit)
A(Mg) dex; axis 7.30–7.73

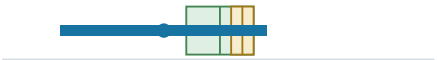
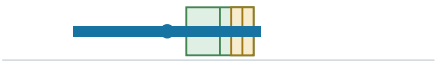
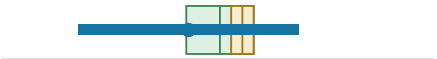
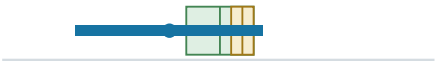
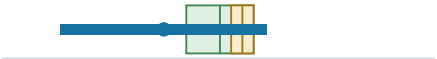
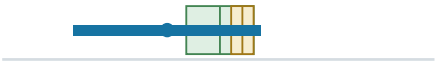
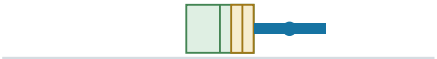
Mg I · Asplund et al. 2021 lines · 1D LTE Reference Grade · 2 lines		7.625 ±0.031
Mg I · Asplund et al. 2021 lines · 3D NLTE (Amarsi) Reference Grade · 2 lines		7.660 ±0.036
Mg I · Asplund et al. 2021 lines · 1D NLTE (Amarsi) Reference Grade · 2 lines		7.625 ±0.031
Mg I · Asplund et al. 2021 lines · 1D NLTE (Gerber) Reference Grade · 2 lines		7.596 ±0.036
Mg I · Asplund et al. 2021 lines · 1D LTE (Gerber) Reference Grade · 2 lines		7.627 ±0.031
Mg I · Deep-graded lines · 1D LTE Deep Grade · 6 lines		7.389 ±0.038
Mg I · Deep-graded lines · 1D NLTE (Amarsi) Deep Grade · 4 lines		7.384 ±0.045

VIS — Kitt Peak (1984, molecfit)
A(Mg) dex; axis 7.30–7.73

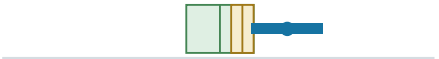
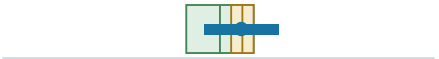
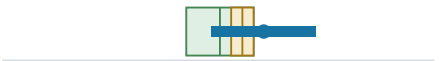
Mg I · Deep-graded lines · 1D NLTE (Gerber) Deep Grade · 6 lines		7.418 ±0.042
Mg I · Deep-graded lines · 1D LTE (Gerber) Deep Grade · 6 lines		7.412 ±0.035
Mg I · Codex-graded lines · 1D LTE Codex Grade · 3 lines		7.617 ±0.059
Mg I · Codex-graded lines · 3D NLTE (Amarsi) Codex Grade · 2 lines		7.660 ±0.036
Mg I · Codex-graded lines · 1D NLTE (Amarsi) Codex Grade · 3 lines		7.617 ±0.069
Mg I · Codex-graded lines · 1D NLTE (Gerber) Codex Grade · 3 lines		7.577 ±0.054
Mg I · Codex-graded lines · 1D LTE (Gerber) Codex Grade · 3 lines		7.619 ±0.059

VIS axis: 7.30 · 7.41 · 7.52 · 7.62 · 7.73 A(Mg) dex

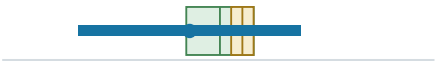
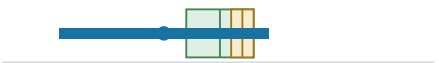
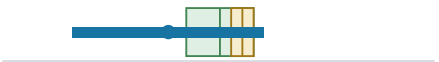
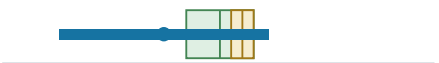
red-optical — IAG FTS
A(Mg) dex; axis 7.36–7.74

Mg II · Asplund et al. 2021 lines · 1D LTE Reference Grade · 2 lines		7.522 ±0.098
Mg II · Asplund et al. 2021 lines · 3D NLTE (Amarsi) Reference Grade · 2 lines		7.505 ±0.084
Mg II · Asplund et al. 2021 lines · 1D NLTE (Amarsi) Reference Grade · 2 lines		7.500 ±0.092
Mg II · Asplund et al. 2021 lines · 1D LTE (Gerber) Reference Grade · 2 lines		7.503 ±0.084
Mg II · Codex-graded lines · 1D LTE Codex Grade · 2 lines		7.522 ±0.098
Mg II · Codex-graded lines · 3D NLTE (Amarsi) Codex Grade · 2 lines		7.505 ±0.084
Mg II · Codex-graded lines · 1D NLTE (Amarsi) Codex Grade · 2 lines		7.500 ±0.092
Mg II · Codex-graded lines · 1D LTE (Gerber) Codex Grade · 2 lines		7.503 ±0.084
Mg I · Asplund et al. 2021 lines · 1D LTE Reference Grade · 3 lines		7.612 ±0.032
Mg I · Asplund et al. 2021 lines · 3D NLTE (Amarsi) Reference Grade · 3 lines		7.661 ±0.041

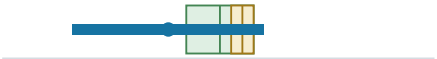
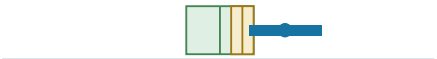
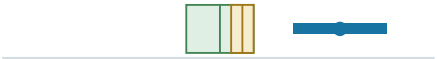
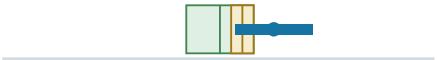
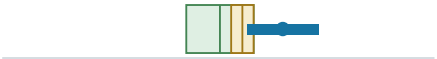
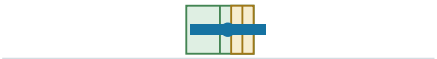
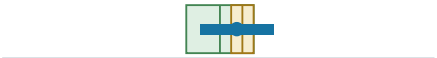
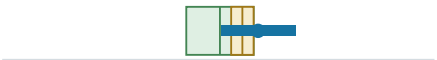
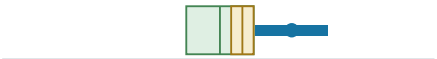
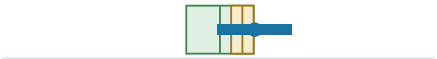
red-optical — IAG FTS
A(Mg) dex; axis 7.36–7.74

Mg I · Asplund et al. 2021 lines · 1D NLTE (Amarsi) Reference Grade · 3 lines		7.611 ±0.032
Mg I · Asplund et al. 2021 lines · 1D NLTE (Gerber) Reference Grade · 3 lines		7.607 ±0.032
Mg I · Asplund et al. 2021 lines · 1D LTE (Gerber) Reference Grade · 3 lines		7.610 ±0.032
SET-MG_BERGEMANN2017 · 1D LTE Reference Grade · 1 line		7.561 ±0.034
SET-MG_BERGEMANN2017 · 1D NLTE (Gerber) Reference Grade · 1 line		7.490 ±0.041
SET-MG_BERGEMANN2017 · 1D LTE (Gerber) Reference Grade · 1 line		7.569 ±0.033
Mg I · Codex-graded lines · 1D LTE Codex Grade · 7 lines		7.591 ±0.047
Mg I · Codex-graded lines · 3D NLTE (Amarsi) Codex Grade · 3 lines		7.671 ±0.040
Mg I · Codex-graded lines · 1D NLTE (Amarsi) Codex Grade · 3 lines		7.618 ±0.032
Mg I · Codex-graded lines · 1D NLTE (Gerber) Codex Grade · 7 lines		7.586 ±0.047
Mg I · Codex-graded lines · 1D LTE (Gerber) Codex Grade · 7 lines		7.589 ±0.046

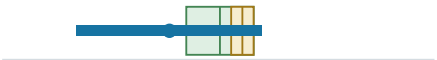
red-optical — Kitt Peak (Kurucz 2005)
A(Mg) dex; axis 7.36–7.74

Mg II · Asplund et al. 2021 lines · 1D LTE Reference Grade · 2 lines		7.523 ±0.099
Mg II · Asplund et al. 2021 lines · 3D NLTE (Amarsi) Reference Grade · 2 lines		7.505 ±0.085
Mg II · Asplund et al. 2021 lines · 1D NLTE (Amarsi) Reference Grade · 2 lines		7.500 ±0.093
Mg II · Asplund et al. 2021 lines · 1D LTE (Gerber) Reference Grade · 2 lines		7.504 ±0.085
Mg II · Codex-graded lines · 1D LTE Codex Grade · 2 lines		7.523 ±0.099
Mg II · Codex-graded lines · 3D NLTE (Amarsi) Codex Grade · 2 lines		7.505 ±0.085
Mg II · Codex-graded lines · 1D NLTE (Amarsi) Codex Grade · 2 lines		7.500 ±0.093

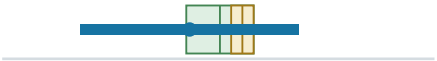
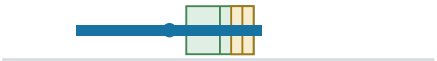
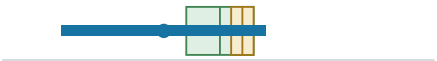
red-optical — Kitt Peak (Kurucz 2005)
A(Mg) dex; axis 7.36–7.74

Mg II · Codex-graded lines · 1D LTE (Gerber) Codex Grade · 2 lines		7.504 ±0.085
Mg I · Asplund et al. 2021 lines · 1D LTE Reference Grade · 3 lines		7.608 ±0.032
Mg I · Asplund et al. 2021 lines · 3D NLTE (Amarsi) Reference Grade · 3 lines		7.657 ±0.042
Mg I · Asplund et al. 2021 lines · 1D NLTE (Amarsi) Reference Grade · 3 lines		7.607 ±0.032
Mg I · Asplund et al. 2021 lines · 1D NLTE (Gerber) Reference Grade · 3 lines		7.598 ±0.034
Mg I · Asplund et al. 2021 lines · 1D LTE (Gerber) Reference Grade · 3 lines		7.606 ±0.032
SET-MG_BERGEMANN2017 · 1D LTE Reference Grade · 1 line		7.557 ±0.034
SET-MG_BERGEMANN2017 · 1D NLTE (Gerber) Reference Grade · 1 line		7.488 ±0.060
SET-MG_BERGEMANN2017 · 1D LTE (Gerber) Reference Grade · 1 line		7.565 ±0.033
Mg I · Codex-graded lines · 1D LTE Codex Grade · 7 lines		7.584 ±0.033
Mg I · Codex-graded lines · 3D NLTE (Amarsi) Codex Grade · 3 lines		7.660 ±0.041
Mg I · Codex-graded lines · 1D NLTE (Amarsi) Codex Grade · 3 lines		7.614 ±0.032
Mg I · Codex-graded lines · 1D NLTE (Gerber) Codex Grade · 7 lines		7.566 ±0.035
Mg I · Codex-graded lines · 1D LTE (Gerber) Codex Grade · 7 lines		7.581 ±0.033

red-optical — Kitt Peak (1984, molecfit)
A(Mg) dex; axis 7.36–7.74

Mg II · Asplund et al. 2021 lines · 1D LTE Reference Grade · 2 lines		7.523 ±0.097
Mg II · Asplund et al. 2021 lines · 3D NLTE (Amarsi) Reference Grade · 2 lines		7.505 ±0.083
Mg II · Asplund et al. 2021 lines · 1D NLTE (Amarsi) Reference Grade · 2 lines		7.500 ±0.091
Mg II · Asplund et al. 2021 lines · 1D LTE (Gerber) Reference Grade · 2 lines		7.502 ±0.082

red-optical — Kitt Peak (1984, molecfit)
A(Mg) dex; axis 7.36–7.74

Mg II · Codex-graded lines · 1D LTE Codex Grade · 2 lines		7.523 ±0.097
Mg II · Codex-graded lines · 3D NLTE (Amarsi) Codex Grade · 2 lines		7.505 ±0.083
Mg II · Codex-graded lines · 1D NLTE (Amarsi) Codex Grade · 2 lines		7.500 ±0.091
Mg II · Codex-graded lines · 1D LTE (Gerber) Codex Grade · 2 lines		7.502 ±0.082
Mg I · Asplund et al. 2021 lines · 1D LTE Reference Grade · 3 lines		7.614 ±0.032
Mg I · Asplund et al. 2021 lines · 3D NLTE (Amarsi) Reference Grade · 3 lines		7.663 ±0.042
Mg I · Asplund et al. 2021 lines · 1D NLTE (Amarsi) Reference Grade · 3 lines		7.613 ±0.032
Mg I · Asplund et al. 2021 lines · 1D NLTE (Gerber) Reference Grade · 3 lines		7.602 ±0.035
Mg I · Asplund et al. 2021 lines · 1D LTE (Gerber) Reference Grade · 3 lines		7.612 ±0.032
SET-MG_BERGEMANN2017 · 1D LTE Reference Grade · 1 line		7.554 ±0.034
SET-MG_BERGEMANN2017 · 1D NLTE (Gerber) Reference Grade · 1 line		7.475 ±0.089
SET-MG_BERGEMANN2017 · 1D LTE (Gerber) Reference Grade · 1 line		7.563 ±0.033
Mg I · Codex-graded lines · 1D LTE Codex Grade · 7 lines		7.576 ±0.035
Mg I · Codex-graded lines · 3D NLTE (Amarsi) Codex Grade · 3 lines		7.666 ±0.041
Mg I · Codex-graded lines · 1D NLTE (Amarsi) Codex Grade · 3 lines		7.620 ±0.032
Mg I · Codex-graded lines · 1D NLTE (Gerber) Codex Grade · 7 lines		7.568 ±0.037
Mg I · Codex-graded lines · 1D LTE (Gerber) Codex Grade · 7 lines		7.573 ±0.035

red-optical axis: 7.36 · 7.45 · 7.55 · 7.64 · 7.74 A(Mg) dex

NIR — CRIRES+ Y (full arm)
A(Mg) dex; axis 7.05–8.10

Mg II · Asplund et al. 2021 lines · 1D LTE Reference Grade · 1 line	7.344 ±0.232
Mg II · Asplund et al. 2021 lines · 3D NLTE (Amarsi) Reference Grade · 1 line	7.321 ±0.233
Mg II · Asplund et al. 2021 lines · 1D NLTE (Amarsi) Reference Grade · 1 line	7.349 ±0.232
Mg II · Asplund et al. 2021 lines · 1D LTE (Gerber) Reference Grade · 1 line	7.306 ±0.225
Mg II · Codex-graded lines · 1D LTE Codex Grade · 1 line	7.344 ±0.232
Mg II · Codex-graded lines · 3D NLTE (Amarsi) Codex Grade · 1 line	7.321 ±0.233
Mg II · Codex-graded lines · 1D NLTE (Amarsi) Codex Grade · 1 line	7.349 ±0.232
Mg II · Codex-graded lines · 1D LTE (Gerber) Codex Grade · 1 line	7.306 ±0.225
Mg I · Asplund et al. 2021 lines · 3D NLTE (Amarsi) Reference Grade · 1 line	7.550 ±0.051
Mg I · Asplund et al. 2021 lines · 1D NLTE (Amarsi) Reference Grade · 1 line	7.514 ±0.047
Mg I · Asplund et al. 2021 lines · 1D LTE (Gerber) Reference Grade · 2 lines	7.607 ±0.151
Mg I · Codex-graded lines · 1D LTE Codex Grade · 1 line	7.514 ±0.047
Mg I · Codex-graded lines · 3D NLTE (Amarsi) Codex Grade · 1 line	7.550 ±0.051
Mg I · Codex-graded lines · 1D NLTE (Amarsi) Codex Grade · 1 line	7.514 ±0.047
Mg I · Codex-graded lines · 1D NLTE (Gerber) Codex Grade · 1 line	7.506 ±0.356
Mg I · Codex-graded lines · 1D LTE (Gerber) Codex Grade · 1 line	7.513 ±0.048

NIR — IAG FTS
A(Mg) dex; axis 7.05–8.10

Mg II · Asplund et al. 2021 lines · 1D LTE Reference Grade · 2 lines	7.725 ±0.156
Mg II · Asplund et al. 2021 lines · 3D NLTE (Amarsi) Reference Grade · 2 lines	7.703 ±0.153

NIR — IAG FTS
A(Mg) dex; axis 7.05–8.10

Mg II · Asplund et al. 2021 lines · 1D NLTE (Amarsi) Reference Grade · 2 lines		7.657 ±0.147
Mg II · Asplund et al. 2021 lines · 1D LTE (Gerber) Reference Grade · 2 lines		7.686 ±0.158
Mg II · Codex-graded lines · 1D LTE Codex Grade · 2 lines		7.725 ±0.156
Mg II · Codex-graded lines · 3D NLTE (Amarsi) Codex Grade · 2 lines		7.703 ±0.153
Mg II · Codex-graded lines · 1D NLTE (Amarsi) Codex Grade · 2 lines		7.657 ±0.147
Mg II · Codex-graded lines · 1D LTE (Gerber) Codex Grade · 2 lines		7.686 ±0.158
Mg I · Asplund et al. 2021 lines · 1D LTE Reference Grade · 1 line		7.649 ±0.086
Mg I · Asplund et al. 2021 lines · 1D NLTE (Gerber) Reference Grade · 1 line		7.640 ±0.104
Mg I · Asplund et al. 2021 lines · 1D LTE (Gerber) Reference Grade · 1 line		7.648 ±0.085
Mg I · Codex-graded lines · 1D LTE Codex Grade · 5 lines		7.586 ±0.111
Mg I · Codex-graded lines · 1D NLTE (Gerber) Codex Grade · 5 lines		7.574 ±0.113
Mg I · Codex-graded lines · 1D LTE (Gerber) Codex Grade · 5 lines		7.584 ±0.112

NIR — Kitt Peak (Kurucz 2005)
A(Mg) dex; axis 7.05–8.10

Mg II · Asplund et al. 2021 lines · 1D LTE Reference Grade · 2 lines		7.879 ±0.186
Mg II · Asplund et al. 2021 lines · 3D NLTE (Amarsi) Reference Grade · 2 lines		7.857 ±0.183
Mg II · Asplund et al. 2021 lines · 1D NLTE (Amarsi) Reference Grade · 2 lines		7.811 ±0.177
Mg II · Asplund et al. 2021 lines · 1D LTE (Gerber) Reference Grade · 2 lines		7.838 ±0.180
Mg II · Codex-graded lines · 1D LTE Codex Grade · 2 lines		7.879 ±0.186
Mg II · Codex-graded lines · 3D NLTE (Amarsi) Codex Grade · 2 lines		7.857 ±0.183

NIR — Kitt Peak (Kurucz 2005)
A(Mg) dex; axis 7.05–8.10

Mg II · Codex-graded lines · 1D NLTE (Amarsi) Codex Grade · 2 lines		7.811 ±0.177
Mg II · Codex-graded lines · 1D LTE (Gerber) Codex Grade · 2 lines		7.838 ±0.180
Mg I · Asplund et al. 2021 lines · 1D LTE Reference Grade · 1 line		7.661 ±0.046
Mg I · Asplund et al. 2021 lines · 1D NLTE (Gerber) Reference Grade · 1 line		7.646 ±0.172
Mg I · Asplund et al. 2021 lines · 1D LTE (Gerber) Reference Grade · 1 line		7.661 ±0.046
Mg I · Codex-graded lines · 1D LTE Codex Grade · 4 lines		7.712 ±0.050
Mg I · Codex-graded lines · 1D NLTE (Gerber) Codex Grade · 4 lines		7.687 ±0.051
Mg I · Codex-graded lines · 1D LTE (Gerber) Codex Grade · 4 lines		7.709 ±0.050

NIR — Kitt Peak (1984, molecfit)
A(Mg) dex; axis 7.05–8.10

Mg II · Asplund et al. 2021 lines · 1D LTE Reference Grade · 4 lines		7.740 ±0.106
Mg II · Asplund et al. 2021 lines · 3D NLTE (Amarsi) Reference Grade · 4 lines		7.717 ±0.106
Mg II · Asplund et al. 2021 lines · 1D NLTE (Amarsi) Reference Grade · 4 lines		7.691 ±0.098
Mg II · Asplund et al. 2021 lines · 1D LTE (Gerber) Reference Grade · 4 lines		7.703 ±0.101
Mg II · Codex-graded lines · 1D LTE Codex Grade · 5 lines		7.637 ±0.097
Mg II · Codex-graded lines · 3D NLTE (Amarsi) Codex Grade · 4 lines		7.646 ±0.108
Mg II · Codex-graded lines · 1D NLTE (Amarsi) Codex Grade · 4 lines		7.638 ±0.100
Mg II · Codex-graded lines · 1D LTE (Gerber) Codex Grade · 5 lines		7.602 ±0.088
Mg I · Asplund et al. 2021 lines · 3D NLTE (Amarsi) Reference Grade · 1 line		7.608 ±0.050
Mg I · Asplund et al. 2021 lines · 1D NLTE (Amarsi) Reference Grade · 1 line		7.572 ±0.047

NIR — Kitt Peak (1984, molecfit)
A(Mg) dex; axis 7.05–8.10

Mg I · Asplund et al. 2021 lines · 1D LTE (Gerber) Reference Grade · 2 lines		7.631 ±0.067
Mg I · Codex-graded lines · 3D NLTE (Amarsi) Codex Grade · 1 line		7.608 ±0.050
Mg I · Codex-graded lines · 1D NLTE (Amarsi) Codex Grade · 1 line		7.572 ±0.047
Mg I · Codex-graded lines · 1D LTE (Gerber) Codex Grade · 13 lines		7.535 ±0.044

NIR — CRIRES+ J
A(Mg) dex; axis 7.05–8.10

SET-MG_BERGEMANN2017 · 1D LTE Reference Grade · 2 lines		7.557 ±0.140
SET-MG_BERGEMANN2017 · 1D NLTE (Gerber) Reference Grade · 2 lines		7.511 ±0.094
SET-MG_BERGEMANN2017 · 1D LTE (Gerber) Reference Grade · 2 lines		7.564 ±0.146
Mg I · Codex-graded lines · 1D LTE Codex Grade · 7 lines		7.504 ±0.083
Mg I · Codex-graded lines · 1D NLTE (Gerber) Codex Grade · 6 lines		7.513 ±0.040
Mg I · Codex-graded lines · 1D LTE (Gerber) Codex Grade · 7 lines		7.504 ±0.090

NIR — CRIRES+ Y
A(Mg) dex; axis 7.05–8.10

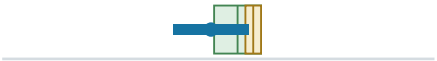
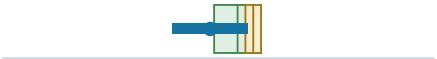
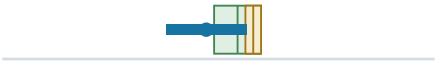
Mg I · Asplund et al. 2021 lines · 1D LTE Reference Grade · 1 line		7.525 ±0.046
Mg I · Asplund et al. 2021 lines · 3D NLTE (Amarsi) Reference Grade · 1 line		7.561 ±0.049
Mg I · Asplund et al. 2021 lines · 1D NLTE (Amarsi) Reference Grade · 1 line		7.525 ±0.046
Mg I · Asplund et al. 2021 lines · 1D NLTE (Gerber) Reference Grade · 1 line		7.527 ±0.417
Mg I · Asplund et al. 2021 lines · 1D LTE (Gerber) Reference Grade · 1 line		7.524 ±0.046

NIR axis: 7.05 · 7.31 · 7.57 · 7.83 · 8.10 A(Mg) dex

H — CRIRES+ H
A(Mg) dex; axis 7.25–7.80

Mg I · Asplund et al. 2021 lines · 1D LTE Reference Grade · 1 line		7.535 ±0.053
Mg I · Asplund et al. 2021 lines · 3D NLTE (Amarsi) Reference Grade · 1 line		7.587 ±0.060
Mg I · Asplund et al. 2021 lines · 1D NLTE (Amarsi) Reference Grade · 1 line		7.534 ±0.053
Mg I · Asplund et al. 2021 lines · 1D NLTE (Gerber) Reference Grade · 1 line		7.527 ±0.170
Mg I · Asplund et al. 2021 lines · 1D LTE (Gerber) Reference Grade · 1 line		7.538 ±0.054
SET-MG_BERGEMANN2017 · 1D LTE (Gerber) Reference Grade · 2 lines		7.561 ±0.211
Mg I · Codex-graded lines · 1D LTE Codex Grade · 8 lines		7.483 ±0.204
Mg I · Codex-graded lines · 1D NLTE (Gerber) Codex Grade · 7 lines		7.569 ±0.138
Mg I · Codex-graded lines · 1D LTE (Gerber) Codex Grade · 9 lines		7.564 ±0.179

H — CRIRES+ H (full arm, telluric-corrected)
A(Mg) dex; axis 7.25–7.80

Mg I · Asplund et al. 2021 lines · 1D LTE Reference Grade · 1 line		7.516 ±0.048
Mg I · Asplund et al. 2021 lines · 3D NLTE (Amarsi) Reference Grade · 1 line		7.568 ±0.055
Mg I · Asplund et al. 2021 lines · 1D NLTE (Amarsi) Reference Grade · 1 line		7.515 ±0.048
Mg I · Asplund et al. 2021 lines · 1D NLTE (Gerber) Reference Grade · 1 line		7.510 ±0.052
Mg I · Asplund et al. 2021 lines · 1D LTE (Gerber) Reference Grade · 1 line		7.519 ±0.048
Mg I · Codex-graded lines · 1D NLTE (Gerber) Codex Grade · 8 lines		7.380 ±0.054
Mg I · Codex-graded lines · 1D LTE (Gerber) Codex Grade · 9 lines		7.446 ±0.056

H axis: 7.25 · 7.39 · 7.53 · 7.66 · 7.80 A(Mg) dex

K — CRIRES+
A(Mg) dex; axis 7.41–7.61

Mg I · Codex-graded lines · 1D LTE Codex Grade · 11 lines		7.502 ±0.067
Mg I · Codex-graded lines · 1D NLTE (Gerber) Codex Grade · 11 lines		7.507 ±0.060
Mg I · Codex-graded lines · 1D LTE (Gerber) Codex Grade · 11 lines		7.508 ±0.067

K axis: 7.41 · 7.46 · 7.51 · 7.56 · 7.61 A(Mg) dex

How to read this forest. Each row is one independent product, preserving its band, holding, engine, indicator and line set. Engines and indicator families are never averaged. Each bar is the uncertainty as Asplund et al. 2021 quote it: line-to-line scatter, the 3D-model term and the NLTE term (at least 0.03 dex). Atomic-data and observational terms are not in the bar, as in Asplund; they stay in the full error budget attached to the row. Grades describe the supplied line-pool provenance, not engine quality; evaluated theoretical CNO oscillator strengths are not relabelled as laboratory evidence. Quarantined, failed and unconstrained fits have no abundance mark. Experimental products remain explicitly not adopted. Literature references provide context, never tuning targets. Yellow rows are Deep Grade: strong lines that saturate, kept but less certain than the other grades.

How this was measured

Every magnesium value on this page comes from fitting synthetic spectra to the observed solar spectrum, line by line or band by band, with the magnesium abundance as the free parameter. The synthesis includes the atomic lines and the molecular opacity in every window, so blended absorption is modelled rather than attributed to the line being measured. The continuum is placed locally around every line by comparing the observation with the synthesis on its own highest pixels, and ground-based spectra are telluric-corrected across their full range.

Each indicator is measured independently on each solar spectrum and reported separately; nothing is averaged across indicators or instruments. Where a 3D or NLTE correction is published for the lines, it is applied as its own product (1D-LTE, 1D-NLTE and 3D-NLTE are separate rows). Every value carries a full uncertainty budget: fit, line strengths, microturbulence, continuum, fit window, model atmosphere, telluric residual, and the spread between spectra, each measured by refitting with that one input changed. The headline at the top is the Asplund-grade product: a published line set, the most complete treatment, then the most lines.

Band	VIS
What was measured	Mg I · Deep-graded lines
Solar spectra	HARPS, Kitt Peak (1984, molecfit), Kitt Peak (Kurucz 2005)
Treatments	1D-LTE, 1D-NLTE
Lines	4–6
Result A(Mg)	7.384–7.472 (1D-NLTE)
Largest uncertainty terms (dex)	fit window 0.11, line strengths (gf) 0.04

Band	VIS
What was measured	Mg I · Codex-graded lines
Solar spectra	HARPS, Kitt Peak (1984, molecfit), Kitt Peak (Kurucz 2005)
Treatments	1D-LTE, 1D-NLTE, 3D-NLTE

Band	VIS
What was measured	Mg I · Codex-graded lines
Lines	2–3
Result A(Mg)	7.646–7.660 (3D-NLTE)
Largest uncertainty terms (dex)	continuum placement 0.08, line strengths (gf) 0.05

Band	VIS
What was measured	Mg I · Asplund et al. 2021 lines
Solar spectra	HARPS, Kitt Peak (1984, molecfit), Kitt Peak (Kurucz 2005)
Treatments	1D-LTE, 1D-NLTE, 3D-NLTE
Lines	2
Result A(Mg)	7.646–7.660 (3D-NLTE)
Largest uncertainty terms (dex)	continuum placement 0.08, line strengths (gf) 0.05

Band	red-optical
What was measured	Mg I · Codex-graded lines; Mg II · Codex-graded lines
Solar spectra	IAG FTS, Kitt Peak (1984, molecfit), Kitt Peak (Kurucz 2005)
Treatments	1D-LTE, 1D-NLTE, 3D-NLTE
Lines	2–7
Result A(Mg)	7.505–7.671 (3D-NLTE)
Largest uncertainty terms (dex)	line strengths (gf) 0.04, NLTE / 3D correction 0.03

Band	red-optical
What was measured	Mg I · Asplund et al. 2021 lines; Mg II · Asplund et al. 2021 lines
Solar spectra	IAG FTS, Kitt Peak (1984, molecfit), Kitt Peak (Kurucz 2005)
Treatments	1D-LTE, 1D-NLTE, 3D-NLTE
Lines	2–3
Result A(Mg)	7.505–7.663 (3D-NLTE)
Largest uncertainty terms (dex)	line strengths (gf) 0.04, NLTE / 3D correction 0.03

Band	red-optical
What was measured	SET-MG_BERGEMANN2017
Solar spectra	IAG FTS, Kitt Peak (1984, molecfit), Kitt Peak (Kurucz 2005)
Treatments	1D-LTE, 1D-NLTE
Lines	1
Result A(Mg)	7.475–7.490 (1D-NLTE)
Largest uncertainty terms (dex)	fit window 0.04, line strengths (gf) 0.03

Band	NIR
What was measured	Mg I · Codex-graded lines; Mg II · Codex-graded lines
Solar spectra	CRIRES+ J, CRIRES+ Y (full arm), IAG FTS, Kitt Peak (1984, molecfit), Kitt Peak (Kurucz 2005)
Treatments	1D-LTE, 1D-NLTE, 3D-NLTE
Lines	1–13
Result A(Mg)	7.321–7.857 (3D-NLTE)
Largest uncertainty terms (dex)	fit / line-to-line scatter 0.10, telluric residual 0.06

Band	NIR
What was measured	Mg I · Asplund et al. 2021 lines; Mg II · Asplund et al. 2021 lines
Solar spectra	CRIRES+ Y, CRIRES+ Y (full arm), IAG FTS, Kitt Peak (1984, molecfit), Kitt Peak (Kurucz 2005)
Treatments	1D-LTE, 1D-NLTE, 3D-NLTE
Lines	1–4
Result A(Mg)	7.321–7.857 (3D-NLTE)
Largest uncertainty terms (dex)	fit / line-to-line scatter 0.10, telluric residual 0.06

Band	NIR
What was measured	SET-MG_BERGEMANN2017
Solar spectra	CRIRES+ J
Treatments	1D-LTE, 1D-NLTE
Lines	2
Result A(Mg)	7.511 (1D-NLTE)
Largest uncertainty terms (dex)	fit window 0.18, fit / line-to-line scatter 0.09

Band	H
What was measured	Mg I · Codex-graded lines
Solar spectra	CRIRES+ H, CRIRES+ H (full arm, telluric-corrected)
Treatments	1D-LTE, 1D-NLTE
Lines	7–9
Result A(Mg)	7.380–7.569 (1D-NLTE)
Largest uncertainty terms (dex)	telluric residual 0.11, fit / line-to-line scatter 0.04

Band	H
What was measured	Mg I · Asplund et al. 2021 lines
Solar spectra	CRIRES+ H, CRIRES+ H (full arm, telluric-corrected)
Treatments	1D-LTE, 1D-NLTE, 3D-NLTE
Lines	1
Result A(Mg)	7.568–7.587 (3D-NLTE)
Largest uncertainty terms (dex)	continuum placement 0.08, line strengths (gf) 0.06

Band	H
What was measured	SET-MG_BERGEMANN2017
Solar spectra	CRIRES+ H
Treatments	1D-LTE
Lines	2
Result A(Mg)	7.561 (1D-LTE)
Largest uncertainty terms (dex)	fit / line-to-line scatter 0.21, telluric residual 0.11

Band	K
What was measured	Mg I · Codex-graded lines
Solar spectra	CRIRES+
Treatments	1D-LTE, 1D-NLTE
Lines	11
Result A(Mg)	7.507 (1D-NLTE)
Largest uncertainty terms (dex)	telluric residual 0.22, fit / line-to-line scatter 0.05

Excluded lines

These lines are left out of the Sun's measurement. They stay in the line lists: a cooler or more evolved star may measure them well. Blended lines are not excluded -- the spectrum synthesis models the blend. 8 lines.

Saturated: on the flat part of the curve of growth, so the line barely responds to the abundance (reduced width log W/λ above -4.9).

Species	Wavelength (Å, air)	Why it is excluded
Mg I	3091.064	saturated
Mg I	3092.985	saturated
Mg I	3096.890	saturated
Mg I	3332.146	saturated
Mg I	3336.674	saturated
Mg I	3627.628	saturated
Mg I	15748.988	atomic_blend
Mg I	24566.296	atomic_blend

Solar magnesium context

Magnesium is measured separately from neutral Mg I and ionized Mg II. Asplund et al. 2021 use eight Mg I and six Mg II features, average the lines within each ion, then weight the two ion means by their total uncertainties. Both ion results are required for the combined abundance.

Published line sets · gf uncertainty model · Methodology

Download the evidence

Download PDF — Solar Mg appendix

Source feed — includes quarantined fit outputs, not adopted abundances

Complete product visibility audit

Shared website/PDF report

Reproducibility manifest

Complete references and product-to-source bindings

Reproducibility

Generated from the pinned science snapshot. Source commit a1130fc6ecc76a2de64f48cb7f9dc6813f9163ce
Feed Mg.json v1.336 · updated 2026-10-29T03:00:33Z
Generated 2026-10-28T21:31:15-06:00 (source commit timestamp)
Feed SHA-256 4541bc29c3c0e7626d31f18a6a09acbcf49f14c87ed09c01510d565cb59cb01e
Generator scripts/generate_cno_publication.py v1.0.0

Pinned scientific source

References / Data & Model Sources

Sources are separated by their role. Registered grid lineage and quarantined diagnostics do not imply an adopted abundance or an applied correction.

See the source notes for the distinction between reference lineage and the treatment actually recorded in each feed entry.

Science and provenance source notes

Solar abundance and indicator analyses. Solar Mg comparison literature; not an adopted Codex abundance. Sources: [1], [2].

Solar abundance and indicator analyses. Published line set MG_AGSS21 (the line selection). Sources: [1].

Atomic data and gf authorities. Mg II oscillator strengths of this pool, as the product's own uncertainty budget records them (with their lineage). Sources: [1].

Model and grid sources. Feed treatment: 1D-LTE synthesis (Turbospectrum); no NLTE/3D correction claimed. Sources: [3].

Model and grid sources. Cited solar abundance differences from the published model columns, applied additively to our LTE fits; not a new in-transfer 3D calculation. Baseline atmosphere: A_marcs_lte Sources: [1].

Model and grid sources. Feed treatment: synth-1D-LTE-gerber; Turbospectrum on the registered Gerber deck. The product retains its own atmosphere and ion identity. Sources: [3].

Atomic data and gf authorities. Mg I oscillator strengths of this pool, as the product's own uncertainty budget records them (with their lineage). Sources: [1].

Model and grid sources. Feed treatment: ENGINE-B-NLTE; Turbospectrum on the registered Gerber deck. The product retains its own atmosphere and ion identity. Sources: [3].

Solar abundance and indicator analyses. Published line set MG_BERGEMANN2017 (the line selection). Sources: [5].

Model and grid sources. Feed treatment: 1D NLTE, per-line correction from the Amarsi 2020 GALAH departure grid via PySME (data/nlte_grids/Mg_Amarsi2020_PySME.csv). Sources: [7].

Product-to-source index

NIR · CRIRES+ Y (full arm) · Mg II · Asplund et al. 2021 lines · 1D LTE · [1], [2], [3] Mg-products-d816dfae18d8

NIR · CRIRES+ Y (full arm) · Mg II · Asplund et al. 2021 lines · 3D NLTE (Amarsi) · [1], [2] Mg-products-6d4fdfbb0d6b

NIR · CRIRES+ Y (full arm) · Mg II · Asplund et al. 2021 lines · 1D NLTE (Amarsi) · [1], [2] Mg-products-afd7d0ed8741

NIR · CRIRES+ Y (full arm) · Mg II · Asplund et al. 2021 lines · 1D LTE (Gerber) · [1], [2], [3] Mg-products-da69d3d9451a

NIR · CRIRES+ Y (full arm) · Mg II · Codex-graded lines · 1D LTE · [1], [2], [3] Mg-products-344fb65a8b45

NIR · CRIRES+ Y (full arm) · Mg II · Codex-graded lines · 3D NLTE (Amarsi) · [1], [2] Mg-products-3ac4e3f1be12

NIR · CRIRES+ Y (full arm) · Mg II · Codex-graded lines · 1D NLTE (Amarsi) · [1], [2] Mg-products-54300e9fa189

NIR · CRIRES+ Y (full arm) · Mg II · Codex-graded lines · 1D LTE (Gerber) · [1], [2], [3] Mg-products-13bb5dae2bce

NIR · IAG FTS · Mg II · Asplund et al. 2021 lines · 1D LTE · [1], [2], [3] Mg-products-ea1cd4c41641

NIR · IAG FTS · Mg II · Asplund et al. 2021 lines · 3D NLTE (Amarsi) · [1], [2] Mg-products-ca8ba673b751

NIR · IAG FTS · Mg II · Asplund et al. 2021 lines · 1D NLTE (Amarsi) · [1], [2] Mg-products-903f351c8958

NIR · IAG FTS · Mg II · Asplund et al. 2021 lines · 1D LTE (Gerber) · [1], [2], [3] Mg-products-6ca87fd6a813

NIR · IAG FTS · Mg II · Codex-graded lines · 1D LTE · [1], [2], [3] Mg-products-b13f93e83939

NIR · IAG FTS · Mg II · Codex-graded lines · 3D NLTE (Amarsi) · [1], [2] Mg-products-20f62e2ec439

NIR · IAG FTS · Mg II · Codex-graded lines · 1D NLTE (Amarsi) · [1], [2] Mg-products-ae878ce2f2be

NIR · IAG FTS · Mg II · Codex-graded lines · 1D LTE (Gerber) · [1], [2], [3] Mg-products-dfb6465cb7e8

NIR · Kitt Peak (Kurucz 2005) · Mg II · Asplund et al. 2021 lines · 1D LTE · [1], [2], [3] Mg-products-702a6c2da144

NIR · Kitt Peak (Kurucz 2005) · Mg II · Asplund et al. 2021 lines · 3D NLTE (Amarsi) · [1], [2] Mg-products-659e1daa958f

NIR · Kitt Peak (Kurucz 2005) · Mg II · Asplund et al. 2021 lines · 1D NLTE (Amarsi) · [1], [2] Mg-products-f0a8686b483e

NIR · Kitt Peak (Kurucz 2005) · Mg II · Asplund et al. 2021 lines · 1D LTE (Gerber) · [1], [2], [3] Mg-products-35cd860a99a9

NIR · Kitt Peak (Kurucz 2005) · Mg II · Codex-graded lines · 1D LTE · [1], [2], [3] Mg-products-1c7f30790e45

NIR · Kitt Peak (Kurucz 2005) · Mg II · Codex-graded lines · 3D NLTE (Amarsi) · [1], [2] Mg-products-42f26154239e

NIR · Kitt Peak (Kurucz 2005) · Mg II · Codex-graded lines · 1D NLTE (Amarsi) · [1], [2] Mg-products-f8756f838b26

NIR · Kitt Peak (Kurucz 2005) · Mg II · Codex-graded lines · 1D LTE (Gerber) · [1], [2], [3] Mg-products-cbd4c0feb814

NIR · Kitt Peak (1984, molecfit) · Mg II · Asplund et al. 2021 lines · 1D LTE · [1], [2], [3] Mg-products-ed210dd16164

NIR · Kitt Peak (1984, molecfit) · Mg II · Asplund et al. 2021 lines · 3D NLTE (Amarsi) · [1], [2] Mg-products-7c66fd4aeff6

NIR · Kitt Peak (1984, molecfit) · Mg II · Asplund et al. 2021 lines · 1D NLTE (Amarsi) · [1], [2] Mg-products-2a1e999b9304

NIR · Kitt Peak (1984, molecfit) · Mg II · Asplund et al. 2021 lines · 1D LTE (Gerber) · [1], [2], [3] Mg-products-10cbfcab6ba1

NIR · Kitt Peak (1984, molecfit) · Mg II · Codex-graded lines · 1D LTE · [1], [2], [4], [3] Mg-products-0c421778989d

NIR · Kitt Peak (1984, molecfit) · Mg II · Codex-graded lines · 3D NLTE (Amarsi) · [1], [2] Mg-products-f3d556522aca

NIR · Kitt Peak (1984, molecfit) · Mg II · Codex-graded lines · 1D NLTE (Amarsi) · [1], [2] Mg-products-0347073ce21a

NIR · Kitt Peak (1984, molecfit) · Mg II · Codex-graded lines · 1D LTE (Gerber) · [1], [2], [4], [3] Mg-products-d7951c973d55

red-optical · IAG FTS · Mg II · Asplund et al. 2021 lines · 1D LTE · [1], [2], [3] Mg-products-1dd951ee1726

red-optical · IAG FTS · Mg II · Asplund et al. 2021 lines · 3D NLTE (Amarsi) · [1], [2] Mg-products-20f801f73171

red-optical · IAG FTS · Mg II · Asplund et al. 2021 lines · 1D NLTE (Amarsi) · [1], [2] Mg-products-3ba978f7f55a

red-optical · IAG FTS · Mg II · Asplund et al. 2021 lines · 1D LTE (Gerber) · [1], [2], [3] Mg-products-31e6081e83c5

red-optical · IAG FTS · Mg II · Codex-graded lines · 1D LTE · [1], [2], [3] Mg-products-0cdb281e368b

red-optical · IAG FTS · Mg II · Codex-graded lines · 3D NLTE (Amarsi) · [1], [2] Mg-products-4e2446414626

red-optical · IAG FTS · Mg II · Codex-graded lines · 1D NLTE (Amarsi) · [1], [2] Mg-products-aae274225071

red-optical · IAG FTS · Mg II · Codex-graded lines · 1D LTE (Gerber) · [1], [2], [3] Mg-products-aafd8e604a79

red-optical · Kitt Peak (Kurucz 2005) · Mg II · Asplund et al. 2021 lines · 1D LTE · [1], [2], [3] Mg-products-7a43f3c277e4

red-optical · Kitt Peak (Kurucz 2005) · Mg II · Asplund et al. 2021 lines · 3D NLTE (Amarsi) · [1], [2] Mg-products-cc94b8a6d134

red-optical · Kitt Peak (Kurucz 2005) · Mg II · Asplund et al. 2021 lines · 1D NLTE (Amarsi) · [1], [2] Mg-products-8fa8852f7e2a

red-optical · Kitt Peak (Kurucz 2005) · Mg II · Asplund et al. 2021 lines · 1D LTE (Gerber) · [1], [2], [3] Mg-products-34746a03d549

red-optical · Kitt Peak (Kurucz 2005) · Mg II · Codex-graded lines · 1D LTE · [1], [2], [3] Mg-products-17f09442f7e6

red-optical · Kitt Peak (Kurucz 2005) · Mg II · Codex-graded lines · 3D NLTE (Amarsi) · [1], [2] Mg-products-b5a5c1f2ac95

red-optical · Kitt Peak (Kurucz 2005) · Mg II · Codex-graded lines · 1D NLTE (Amarsi) · [1], [2] Mg-products-1b9a6621dea3

red-optical · Kitt Peak (Kurucz 2005) · Mg II · Codex-graded lines · 1D LTE (Gerber) · [1], [2], [3] Mg-products-5f2671c15bd8

red-optical · Kitt Peak (1984, molecfit) · Mg II · Asplund et al. 2021 lines · 1D LTE · [1], [2], [3] Mg-products-911ef4bf1468

red-optical · Kitt Peak (1984, molecfit) · Mg II · Asplund et al. 2021 lines · 3D NLTE (Amarsi) · [1], [2] Mg-products-65b76ab79e04

red-optical · Kitt Peak (1984, molecfit) · Mg II · Asplund et al. 2021 lines · 1D NLTE (Amarsi) · [1], [2] Mg-products-0ecdffd59ea4

red-optical · Kitt Peak (1984, molecfit) · Mg II · Asplund et al. 2021 lines · 1D LTE (Gerber) · [1], [2], [3] Mg-products-a6186c9fc963

red-optical · Kitt Peak (1984, molecfit) · Mg II · Codex-graded lines · 1D LTE · [1], [2], [3] Mg-products-1d51ca2f1b5d

red-optical · Kitt Peak (1984, molecfit) · Mg II · Codex-graded lines · 3D NLTE (Amarsi) · [1], [2] Mg-products-07759a54b7dc

red-optical · Kitt Peak (1984, molecfit) · Mg II · Codex-graded lines · 1D NLTE (Amarsi) · [1], [2] Mg-products-cef04b747242

red-optical · Kitt Peak (1984, molecfit) · Mg II · Codex-graded lines · 1D LTE (Gerber) · [1], [2], [3] Mg-products-a5e183d45653

H · CRIRES+ H · Mg I · Asplund et al. 2021 lines · 1D LTE · [1], [2], [3] Mg-products-188616968ca2

H · CRIRES+ H · Mg I · Asplund et al. 2021 lines · 3D NLTE (Amarsi) · [1], [2] Mg-products-7e1670a5bc6c

H · CRIRES+ H · Mg I · Asplund et al. 2021 lines · 1D NLTE (Amarsi) · [1], [2] Mg-products-592c469f5209

H · CRIRES+ H · Mg I · Asplund et al. 2021 lines · 1D NLTE (Gerber) · [1], [2], [3] Mg-products-3f87770aa8c6

H · CRIRES+ H · Mg I · Asplund et al. 2021 lines · 1D LTE (Gerber) · [1], [2], [3] Mg-products-ac15d5c4dfc3

H · CRIRES+ H · SET-MG_BERGEMANN2017 · 1D LTE (Gerber) · [1], [2], [5], [6], [3] Mg-products-bd82a847d3a4

H · CRIRES+ H · Mg I · Codex-graded lines · 1D LTE · [1], [2], [6], [4], [3] Mg-products-ecc90e1d03f1

H · CRIRES+ H · Mg I · Codex-graded lines · 1D NLTE (Gerber) · [1], [2], [6], [4], [3] Mg-products-62cea4ac2c59

H · CRIRES+ H · Mg I · Codex-graded lines · 1D LTE (Gerber) · [1], [2], [6], [4], [3] Mg-products-e91ea5062469

H · CRIRES+ H (full arm, telluric-corrected) · Mg I · Asplund et al. 2021 lines · 1D LTE · [1], [2], [3] Mg-products-d000c5ce6b85

H · CRIRES+ H (full arm, telluric-corrected) · Mg I · Asplund et al. 2021 lines · 3D NLTE (Amarsi) · [1], [2] Mg-products-f99801b5ba1b

H · CRIRES+ H (full arm, telluric-corrected) · Mg I · Asplund et al. 2021 lines · 1D NLTE (Amarsi) · [1], [2] Mg-products-81d206179460

H · CRIRES+ H (full arm, telluric-corrected) · Mg I · Asplund et al. 2021 lines · 1D NLTE (Gerber) · [1], [2], [3] Mg-products-10597f41c021

H · CRIRES+ H (full arm, telluric-corrected) · Mg I · Asplund et al. 2021 lines · 1D LTE (Gerber) · [1], [2], [3] Mg-products-ce8db0d66041

H · CRIRES+ H (full arm, telluric-corrected) · Mg I · Codex-graded lines · 1D NLTE (Gerber) · [1], [2], [6], [4], [5], [3] Mg-products-d8bb5b97cc7e

H · CRIRES+ H (full arm, telluric-corrected) · Mg I · Codex-graded lines · 1D LTE (Gerber) · [1], [2], [6], [4], [5], [3] Mg-products-1909b40189b8

K · CRIRES+ · Mg I · Codex-graded lines · 1D LTE · [1], [2], [4], [3] Mg-products-99de8cd7cbcc

K · CRIRES+ · Mg I · Codex-graded lines · 1D NLTE (Gerber) · [1], [2], [4], [3] Mg-products-3815e328ddc4

K · CRIRES+ · Mg I · Codex-graded lines · 1D LTE (Gerber) · [1], [2], [4], [3] Mg-products-275eece75f99

NIR · CRIRES+ J · SET-MG_BERGEMANN2017 · 1D LTE · [1], [2], [5], [6], [3] Mg-products-f8f393f28370

NIR · CRIRES+ J · SET-MG_BERGEMANN2017 · 1D NLTE (Gerber) · [1], [2], [5], [6], [3] Mg-products-84060533653f

NIR · CRIRES+ J · SET-MG_BERGEMANN2017 · 1D LTE (Gerber) · [1], [2], [5], [6], [3] Mg-products-07cae91a52f9

NIR · CRIRES+ J · Mg I · Codex-graded lines · 1D LTE · [1], [2], [4], [6], [3] Mg-products-c03040e070f0

NIR · CRIRES+ J · Mg I · Codex-graded lines · 1D NLTE (Gerber) · [1], [2], [6], [4], [3] Mg-products-6c343e995cfa

NIR · CRIRES+ J · Mg I · Codex-graded lines · 1D LTE (Gerber) · [1], [2], [4], [6], [3] Mg-products-da24809844c2

NIR · CRIRES+ Y · Mg I · Asplund et al. 2021 lines · 1D LTE · [1], [2], [3] Mg-products-49eb24c3495c

NIR · CRIRES+ Y · Mg I · Asplund et al. 2021 lines · 3D NLTE (Amarsi) · [1], [2] Mg-products-21d94165adac

NIR · CRIRES+ Y · Mg I · Asplund et al. 2021 lines · 1D NLTE (Amarsi) · [1], [2] Mg-products-a35633649cd9

NIR · CRIRES+ Y · Mg I · Asplund et al. 2021 lines · 1D NLTE (Gerber) · [1], [2], [3] Mg-products-39039bd84318

NIR · CRIRES+ Y · Mg I · Asplund et al. 2021 lines · 1D LTE (Gerber) · [1], [2], [3] Mg-products-e02bda0de567

NIR · CRIRES+ Y (full arm) · Mg I · Asplund et al. 2021 lines · 3D NLTE (Amarsi) · [1], [2] Mg-products-3e2ab2c305c1

NIR · CRIRES+ Y (full arm) · Mg I · Asplund et al. 2021 lines · 1D NLTE (Amarsi) · [1], [2] Mg-products-35b746de3e52

NIR · CRIRES+ Y (full arm) · Mg I · Asplund et al. 2021 lines · 1D LTE (Gerber) · [1], [2], [3] Mg-products-67679071c2b6

NIR · CRIRES+ Y (full arm) · Mg I · Codex-graded lines · 1D LTE · [1], [2], [3] Mg-products-476cbbf482f3

NIR · CRIRES+ Y (full arm) · Mg I · Codex-graded lines · 3D NLTE (Amarsi) · [1], [2] Mg-products-c66ff6d91045

NIR · CRIRES+ Y (full arm) · Mg I · Codex-graded lines · 1D NLTE (Amarsi) · [1], [2] Mg-products-2cbaaaf5d30e

NIR · CRIRES+ Y (full arm) · Mg I · Codex-graded lines · 1D NLTE (Gerber) · [1], [2], [3] Mg-products-048ff49242dd

NIR · CRIRES+ Y (full arm) · Mg I · Codex-graded lines · 1D LTE (Gerber) · [1], [2], [3] Mg-products-a2f38d3445a1

NIR · IAG FTS · Mg I · Asplund et al. 2021 lines · 1D LTE · [1], [2], [3] Mg-products-4d4e9a277be8

NIR · IAG FTS · Mg I · Asplund et al. 2021 lines · 1D NLTE (Gerber) · [1], [2], [3] Mg-products-1f2cdb8ac458

NIR · IAG FTS · Mg I · Asplund et al. 2021 lines · 1D LTE (Gerber) · [1], [2], [3] Mg-products-90c5d687a59b

NIR · IAG FTS · Mg I · Codex-graded lines · 1D LTE · [1], [2], [4], [6], [3] Mg-products-ab59ff5768fd

NIR · IAG FTS · Mg I · Codex-graded lines · 1D NLTE (Gerber) · [1], [2], [4], [6], [3] Mg-products-8e5ad708074f

NIR · IAG FTS · Mg I · Codex-graded lines · 1D LTE (Gerber) · [1], [2], [4], [6], [3] Mg-products-ea0ee54ea759

NIR · Kitt Peak (Kurucz 2005) · Mg I · Asplund et al. 2021 lines · 1D LTE · [1], [2], [3] Mg-products-56b9cee76fcd

NIR · Kitt Peak (Kurucz 2005) · Mg I · Asplund et al. 2021 lines · 1D NLTE (Gerber) · [1], [2], [3] Mg-products-9100e741695c

NIR · Kitt Peak (Kurucz 2005) · Mg I · Asplund et al. 2021 lines · 1D LTE (Gerber) · [1], [2], [3] Mg-products-0bd811bed24e

NIR · Kitt Peak (Kurucz 2005) · Mg I · Codex-graded lines · 1D LTE · [1], [2], [6], [4], [3] Mg-products-643f43b2cc04

NIR · Kitt Peak (Kurucz 2005) · Mg I · Codex-graded lines · 1D NLTE (Gerber) · [1], [2], [6], [4], [3] Mg-products-7a3dcd7b98aa

NIR · Kitt Peak (Kurucz 2005) · Mg I · Codex-graded lines · 1D LTE (Gerber) · [1], [2], [6], [4], [3] Mg-products-9d0180e23158

NIR · Kitt Peak (1984, molecfit) · Mg I · Asplund et al. 2021 lines · 3D NLTE (Amarsi) · [1], [2] Mg-products-e8490b8269f6

NIR · Kitt Peak (1984, molecfit) · Mg I · Asplund et al. 2021 lines · 1D NLTE (Amarsi) · [1], [2] Mg-products-9edf762d80c4

NIR · Kitt Peak (1984, molecfit) · Mg I · Asplund et al. 2021 lines · 1D LTE (Gerber) · [1], [2], [3] Mg-products-48a1b81b0b57

NIR · Kitt Peak (1984, molecfit) · Mg I · Codex-graded lines · 3D NLTE (Amarsi) · [1], [2] Mg-products-3f2e7d21bb9d

NIR · Kitt Peak (1984, molecfit) · Mg I · Codex-graded lines · 1D NLTE (Amarsi) · [1], [2] Mg-products-f631a82c728e

NIR · Kitt Peak (1984, molecfit) · Mg I · Codex-graded lines · 1D LTE (Gerber) · [1], [2], [6], [4], [3] Mg-products-f2232bce3c27

VIS · HARPS · Mg I · Asplund et al. 2021 lines · 1D LTE · [1], [2], [3] Mg-products-8771ce27433e

VIS · HARPS · Mg I · Asplund et al. 2021 lines · 3D NLTE (Amarsi) · [1], [2] Mg-products-625d514c9752

VIS · HARPS · Mg I · Asplund et al. 2021 lines · 1D NLTE (Amarsi) · [1], [2] Mg-products-010b8e83ddb0

VIS · HARPS · Mg I · Asplund et al. 2021 lines · 1D NLTE (Gerber) · [1], [2], [3] Mg-products-2c00eba7fd54

VIS · HARPS · Mg I · Asplund et al. 2021 lines · 1D LTE (Gerber) · [1], [2], [3] Mg-products-fff8b029531a

VIS · HARPS · Mg I · Deep-graded lines · 1D LTE · [1], [2], [5], [6], [3] Mg-products-9e9ca5224ad4

VIS · HARPS · Mg I · Deep-graded lines · 1D NLTE (Amarsi) · [1], [2], [5], [6], [7] Mg-products-26ad0da45e60

VIS · HARPS · Mg I · Deep-graded lines · 1D NLTE (Gerber) · [1], [2], [5], [6], [3] Mg-products-281471766b3f

VIS · HARPS · Mg I · Deep-graded lines · 1D LTE (Gerber) · [1], [2], [5], [6], [3] Mg-products-80e3352427f0

VIS · HARPS · Mg I · Codex-graded lines · 1D LTE · [1], [2], [5], [3] Mg-products-dec40986e5ce

VIS · HARPS · Mg I · Codex-graded lines · 3D NLTE (Amarsi) · [1], [2] Mg-products-3677c36e9e6b

VIS · HARPS · Mg I · Codex-graded lines · 1D NLTE (Amarsi) · [1], [2], [5] Mg-products-991705b37a93

VIS · HARPS · Mg I · Codex-graded lines · 1D NLTE (Gerber) · [1], [2], [5], [3] Mg-products-51aca9f1e3aa

VIS · HARPS · Mg I · Codex-graded lines · 1D LTE (Gerber) · [1], [2], [5], [3] Mg-products-c0b3b7abc270

VIS · Kitt Peak (Kurucz 2005) · Mg I · Asplund et al. 2021 lines · 1D LTE · [1], [2], [3] Mg-products-1d5e4ebe23df

VIS · Kitt Peak (Kurucz 2005) · Mg I · Asplund et al. 2021 lines · 3D NLTE (Amarsi) · [1], [2] Mg-products-bfebaffec2f9

VIS · Kitt Peak (Kurucz 2005) · Mg I · Asplund et al. 2021 lines · 1D NLTE (Amarsi) · [1], [2] Mg-products-f2cff51673d7

VIS · Kitt Peak (Kurucz 2005) · Mg I · Asplund et al. 2021 lines · 1D NLTE (Gerber) · [1], [2], [3] Mg-products-a213d509739f

VIS · Kitt Peak (Kurucz 2005) · Mg I · Asplund et al. 2021 lines · 1D LTE (Gerber) · [1], [2], [3] Mg-products-23b175882060

VIS · Kitt Peak (Kurucz 2005) · Mg I · Deep-graded lines · 1D LTE · [1], [2], [5], [6], [3] Mg-products-c3b9afb3b77d

VIS · Kitt Peak (Kurucz 2005) · Mg I · Deep-graded lines · 1D NLTE (Amarsi) · [1], [2], [5], [6], [7] Mg-products-cd7a8de589c5

VIS · Kitt Peak (Kurucz 2005) · Mg I · Deep-graded lines · 1D NLTE (Gerber) · [1], [2], [5], [6], [3] Mg-products-26302d1bc29a

VIS · Kitt Peak (Kurucz 2005) · Mg I · Deep-graded lines · 1D LTE (Gerber) · [1], [2], [5], [6], [3] Mg-products-0aefd96d693c

VIS · Kitt Peak (Kurucz 2005) · Mg I · Codex-graded lines · 1D LTE · [1], [2], [5], [3] Mg-products-17cd8f1e4f9b

VIS · Kitt Peak (Kurucz 2005) · Mg I · Codex-graded lines · 3D NLTE (Amarsi) · [1], [2] Mg-products-f14df3dc373e

VIS · Kitt Peak (Kurucz 2005) · Mg I · Codex-graded lines · 1D NLTE (Amarsi) · [1], [2], [5] Mg-products-a538e6cb9c03

VIS · Kitt Peak (Kurucz 2005) · Mg I · Codex-graded lines · 1D NLTE (Gerber) · [1], [2], [5], [3] Mg-products-a46f3c184042

VIS · Kitt Peak (Kurucz 2005) · Mg I · Codex-graded lines · 1D LTE (Gerber) · [1], [2], [5], [3] Mg-products-4c9675f0eca3

VIS · Kitt Peak (1984, molecfit) · Mg I · Asplund et al. 2021 lines · 1D LTE · [1], [2], [3] Mg-products-c4d9244b5196

VIS · Kitt Peak (1984, molecfit) · Mg I · Asplund et al. 2021 lines · 3D NLTE (Amarsi) · [1], [2] Mg-products-133fb9ecd813

VIS · Kitt Peak (1984, molecfit) · Mg I · Asplund et al. 2021 lines · 1D NLTE (Amarsi) · [1], [2] Mg-products-eda9997003ae

VIS · Kitt Peak (1984, molecfit) · Mg I · Asplund et al. 2021 lines · 1D NLTE (Gerber) · [1], [2], [3] Mg-products-46ea9e7fd171

VIS · Kitt Peak (1984, molecfit) · Mg I · Asplund et al. 2021 lines · 1D LTE (Gerber) · [1], [2], [3] Mg-products-982c9e0668ac

VIS · Kitt Peak (1984, molecfit) · Mg I · Deep-graded lines · 1D LTE · [1], [2], [5], [6], [3] Mg-products-04b861548e37

VIS · Kitt Peak (1984, molecfit) · Mg I · Deep-graded lines · 1D NLTE (Amarsi) · [1], [2], [5], [6], [7] Mg-products-baa64f92eebf

VIS · Kitt Peak (1984, molecfit) · Mg I · Deep-graded lines · 1D NLTE (Gerber) · [1], [2], [5], [6], [3] Mg-products-dc05e267565e

VIS · Kitt Peak (1984, molecfit) · Mg I · Deep-graded lines · 1D LTE (Gerber) · [1], [2], [5], [6], [3] Mg-products-05a2025db5a7

VIS · Kitt Peak (1984, molecfit) · Mg I · Codex-graded lines · 1D LTE · [1], [2], [5], [3] Mg-products-0b2abc5e47a0

VIS · Kitt Peak (1984, molecfit) · Mg I · Codex-graded lines · 3D NLTE (Amarsi) · [1], [2] Mg-products-735f226693c4

VIS · Kitt Peak (1984, molecfit) · Mg I · Codex-graded lines · 1D NLTE (Amarsi) · [1], [2], [5] Mg-products-78d23bd083cd

VIS · Kitt Peak (1984, molecfit) · Mg I · Codex-graded lines · 1D NLTE (Gerber) · [1], [2], [5], [3] Mg-products-9c0b11524f4c

VIS · Kitt Peak (1984, molecfit) · Mg I · Codex-graded lines · 1D LTE (Gerber) · [1], [2], [5], [3] Mg-products-c273a9e5bac8

red-optical · IAG FTS · Mg I · Asplund et al. 2021 lines · 1D LTE · [1], [2], [3] Mg-products-3a9822e1b5f0

red-optical · IAG FTS · Mg I · Asplund et al. 2021 lines · 3D NLTE (Amarsi) · [1], [2] Mg-products-94820bea5344

red-optical · IAG FTS · Mg I · Asplund et al. 2021 lines · 1D NLTE (Amarsi) · [1], [2] Mg-products-61b8829b28bd

red-optical · IAG FTS · Mg I · Asplund et al. 2021 lines · 1D NLTE (Gerber) · [1], [2], [3] Mg-products-03b0c784b0ff

red-optical · IAG FTS · Mg I · Asplund et al. 2021 lines · 1D LTE (Gerber) · [1], [2], [3] Mg-products-4ab4aa46fe16

red-optical · IAG FTS · SET-MG_BERGEMANN2017 · 1D LTE · [1], [2], [5], [6], [3] Mg-products-d1524a7420c0

red-optical · IAG FTS · SET-MG_BERGEMANN2017 · 1D NLTE (Gerber) · [1], [2], [5], [6], [3] Mg-products-f3cf7b3f9509

red-optical · IAG FTS · SET-MG_BERGEMANN2017 · 1D LTE (Gerber) · [1], [2], [5], [6], [3] Mg-products-ffcd6c5700fe

red-optical · IAG FTS · Mg I · Codex-graded lines · 1D LTE · [1], [2], [6], [3] Mg-products-aef7b639497a

red-optical · IAG FTS · Mg I · Codex-graded lines · 3D NLTE (Amarsi) · [1], [2] Mg-products-c877b576d78e

red-optical · IAG FTS · Mg I · Codex-graded lines · 1D NLTE (Amarsi) · [1], [2] Mg-products-8b548ef6e701

red-optical · IAG FTS · Mg I · Codex-graded lines · 1D NLTE (Gerber) · [1], [2], [6], [3] Mg-products-49986f5fee71

red-optical · IAG FTS · Mg I · Codex-graded lines · 1D LTE (Gerber) · [1], [2], [6], [3] Mg-products-6eea4503bc94

red-optical · Kitt Peak (Kurucz 2005) · Mg I · Asplund et al. 2021 lines · 1D LTE · [1], [2], [3] Mg-products-07f98bb5f7db

red-optical · Kitt Peak (Kurucz 2005) · Mg I · Asplund et al. 2021 lines · 3D NLTE (Amarsi) · [1], [2] Mg-products-31220369b3ac

red-optical · Kitt Peak (Kurucz 2005) · Mg I · Asplund et al. 2021 lines · 1D NLTE (Amarsi) · [1], [2] Mg-products-39f66723fca7

red-optical · Kitt Peak (Kurucz 2005) · Mg I · Asplund et al. 2021 lines · 1D NLTE (Gerber) · [1], [2], [3] Mg-products-0ee7da7b6b2f

red-optical · Kitt Peak (Kurucz 2005) · Mg I · Asplund et al. 2021 lines · 1D LTE (Gerber) · [1], [2], [3] Mg-products-e84549ad4659

red-optical · Kitt Peak (Kurucz 2005) · SET-MG_BERGEMANN2017 · 1D LTE · [1], [2], [5], [6], [3] Mg-products-2ff6d4c90db9

red-optical · Kitt Peak (Kurucz 2005) · SET-MG_BERGEMANN2017 · 1D NLTE (Gerber) · [1], [2], [5], [6], [3] Mg-products-9b8f9cc32dcf

red-optical · Kitt Peak (Kurucz 2005) · SET-MG_BERGEMANN2017 · 1D LTE (Gerber) · [1], [2], [5], [6], [3] Mg-products-c4b8a45ce618

red-optical · Kitt Peak (Kurucz 2005) · Mg I · Codex-graded lines · 1D LTE · [1], [2], [6], [3] Mg-products-d86a20c2e9b2

red-optical · Kitt Peak (Kurucz 2005) · Mg I · Codex-graded lines · 3D NLTE (Amarsi) · [1], [2] Mg-products-af1aa9c94021

red-optical · Kitt Peak (Kurucz 2005) · Mg I · Codex-graded lines · 1D NLTE (Amarsi) · [1], [2] Mg-products-d1ee172898d5

red-optical · Kitt Peak (Kurucz 2005) · Mg I · Codex-graded lines · 1D NLTE (Gerber) · [1], [2], [6], [3] Mg-products-fc1e6d152e2f

red-optical · Kitt Peak (Kurucz 2005) · Mg I · Codex-graded lines · 1D LTE (Gerber) · [1], [2], [6], [3] Mg-products-3a6227513319

red-optical · Kitt Peak (1984, molecfit) · Mg I · Asplund et al. 2021 lines · 1D LTE · [1], [2], [3] Mg-products-c2df4b32cfa8

red-optical · Kitt Peak (1984, molecfit) · Mg I · Asplund et al. 2021 lines · 3D NLTE (Amarsi) · [1], [2] Mg-products-d239977327a6

red-optical · Kitt Peak (1984, molecfit) · Mg I · Asplund et al. 2021 lines · 1D NLTE (Amarsi) · [1], [2] Mg-products-55a63ea4c654

red-optical · Kitt Peak (1984, molecfit) · Mg I · Asplund et al. 2021 lines · 1D NLTE (Gerber) · [1], [2], [3] Mg-products-f62719caf89e

red-optical · Kitt Peak (1984, molecfit) · Mg I · Asplund et al. 2021 lines · 1D LTE (Gerber) · [1], [2], [3] Mg-products-bf2039181f20

red-optical · Kitt Peak (1984, molecfit) · SET-MG_BERGEMANN2017 · 1D LTE · [1], [2], [5], [6], [3] Mg-products-282f16bdbfa1

red-optical · Kitt Peak (1984, molecfit) · SET-MG_BERGEMANN2017 · 1D NLTE (Gerber) · [1], [2], [5], [6], [3] Mg-products-7186aca05cc9

red-optical · Kitt Peak (1984, molecfit) · SET-MG_BERGEMANN2017 · 1D LTE (Gerber) · [1], [2], [5], [6], [3] Mg-products-897552a607c5

red-optical · Kitt Peak (1984, molecfit) · Mg I · Codex-graded lines · 1D LTE · [1], [2], [6], [3] Mg-products-d0ccb0998ca8

red-optical · Kitt Peak (1984, molecfit) · Mg I · Codex-graded lines · 3D NLTE (Amarsi) · [1], [2] Mg-products-ee8a60588a28

red-optical · Kitt Peak (1984, molecfit) · Mg I · Codex-graded lines · 1D NLTE (Amarsi) · [1], [2] Mg-products-cbbf337e7e1b

red-optical · Kitt Peak (1984, molecfit) · Mg I · Codex-graded lines · 1D NLTE (Gerber) · [1], [2], [6], [3] Mg-products-6e5932a8db83

red-optical · Kitt Peak (1984, molecfit) · Mg I · Codex-graded lines · 1D LTE (Gerber) · [1], [2], [6], [3] Mg-products-42c06b39b917

VIS · Kitt Peak (Kurucz 2005) · SET-MG_BERGEMANN2017 · 1D LTE (Gerber) · [1], [2], [5], [6], [3] Mg-quarantine-b52d72dd9990

VIS · Kitt Peak (Kurucz 2005) · SET-MG_BERGEMANN2017 · 1D NLTE (Gerber) · [1], [2], [5], [6], [3] Mg-quarantine-8643f7bb20af

VIS · Kitt Peak (Kurucz 2005) · SET-MG_BERGEMANN2017 · 1D LTE · [1], [2], [5], [6], [3] Mg-quarantine-1a1af53a4420

VIS · Kitt Peak (Kurucz 2005) · SET-MG_BERGEMANN2017 · 1D NLTE (Amarsi) · [1], [2], [5], [6], [7] Mg-quarantine-5afeb6e574ca

VIS · Kitt Peak (1984, molecfit) · SET-MG_BERGEMANN2017 · 1D LTE (Gerber) · [1], [2], [5], [6], [3] Mg-quarantine-36b43478e36a

VIS · Kitt Peak (1984, molecfit) · SET-MG_BERGEMANN2017 · 1D NLTE (Gerber) · [1], [2], [5], [6], [3] Mg-quarantine-93d9594958c1

VIS · Kitt Peak (1984, molecfit) · SET-MG_BERGEMANN2017 · 1D LTE · [1], [2], [5], [6], [3] Mg-quarantine-4e9f22e2a3b0

VIS · Kitt Peak (1984, molecfit) · SET-MG_BERGEMANN2017 · 1D NLTE (Amarsi) · [1], [2], [5], [6], [7] Mg-quarantine-8edced6ff6e1

VIS · HARPS · SET-MG_BERGEMANN2017 · 1D LTE (Gerber) · [1], [2], [5], [6], [3] Mg-quarantine-f25842530f9a

VIS · HARPS · SET-MG_BERGEMANN2017 · 1D NLTE (Gerber) · [1], [2], [5], [6], [3] Mg-quarantine-b3a8eca5cdb8

VIS · HARPS · SET-MG_BERGEMANN2017 · 1D LTE · [1], [2], [5], [6], [3] Mg-quarantine-3b5e57d664fb

VIS · HARPS · SET-MG_BERGEMANN2017 · 1D NLTE (Amarsi) · [1], [2], [5], [6], [7] Mg-quarantine-182e08af1233

NIR · Kitt Peak (1984, molecfit) · SET-MG_BERGEMANN2017 · 1D LTE (Gerber) · [1], [2], [5], [6], [3] Mg-quarantine-74110dd170d0

NIR · Kitt Peak (1984, molecfit) · Mg I · Codex-graded lines · 1D NLTE (Gerber) · [1], [2], [6], [4], [3] Mg-quarantine-ed8a22bc135b

NIR · Kitt Peak (1984, molecfit) · Mg I · Asplund et al. 2021 lines · 1D NLTE (Gerber) · [1], [2], [3] Mg-quarantine-da22d8adab31

NIR · Kitt Peak (1984, molecfit) · SET-MG_BERGEMANN2017 · 1D NLTE (Gerber) · [1], [2], [5], [6], [3] Mg-quarantine-c0fc0f5dd738

NIR · Kitt Peak (1984, molecfit) · Mg I · Codex-graded lines · 1D LTE · [1], [2], [6], [4], [3] Mg-quarantine-9b9fe8bbfe3e

NIR · Kitt Peak (1984, molecfit) · Mg I · Asplund et al. 2021 lines · 1D LTE · [1], [2], [3] Mg-quarantine-adb3dfe1171e

NIR · Kitt Peak (1984, molecfit) · SET-MG_BERGEMANN2017 · 1D LTE · [1], [2], [5], [6], [3] Mg-quarantine-e06e523c799c

NIR · CRIRES+ Y (full arm) · Mg I · Asplund et al. 2021 lines · 1D NLTE (Gerber) · [1], [2], [3] Mg-quarantine-bdcc0243b7a9

NIR · CRIRES+ Y (full arm) · Mg I · Asplund et al. 2021 lines · 1D LTE · [1], [2], [3] Mg-quarantine-60c9f0540677

H · CRIRES+ H · SET-MG_BERGEMANN2017 · 1D NLTE (Gerber) · [1], [2], [5], [6], [3] Mg-quarantine-43a66451f55f

H · CRIRES+ H (full arm, telluric-corrected) · SET-MG_BERGEMANN2017 · 1D LTE (Gerber) · [1], [2], [5], [6], [3] Mg-quarantine-cfec46cea0cf

H · CRIRES+ H (full arm, telluric-corrected) · SET-MG_BERGEMANN2017 · 1D NLTE (Gerber) · [1], [2], [5], [6], [3] Mg-quarantine-5ed77bdd362a

Complete applicable bibliography

Solar abundance and indicator analyses

[1] — Asplund, M.; Amarsi, A. M.; Grevesse, N. (2021). The chemical make-up of the Sun: A 2020 vision. A&A 653, A141 DOI: 10.1051/0004-6361/202140445. source record

[2] — Lodders, K.; Bergemann, M.; Palme, H. (2025). Solar System Elemental Abundances from the Solar Photosphere and CI-Chondrites. Space Science Reviews 221 DOI: 10.1007/s11214-025-01146-w. source record

[5] — Bergemann, M.; Collet, R.; Amarsi, A. M.; Kovalev, M.; Ruchti, G.; Magic, Z. (2017). Non-local Thermodynamic Equilibrium Stellar Spectroscopy with 1D and <3D> Models. I. Methods and Application to Magnesium Abundances in Standard Stars. ApJ 847, 15 DOI: 10.3847/1538-4357/aa88cb. source record

Atomic data and gf authorities

[4] — Kramida, A.; Ralchenko, Yu.; Reader, J.; NIST ASD Team (2024). NIST Atomic Spectra Database (version 5.11/5.12). National Institute of Standards and Technology, Gaithersburg, MD DOI: 10.18434/T4W30F. source record

[6] — Pehlivan Rhodin, A.; Hartman, H.; Nilsson, H.; Jonsson, P. (2017). Experimental and theoretical oscillator strengths of Mg I for accurate abundance analysis. A&A 598, A102 DOI: 10.1051/0004-6361/201629849. source record

Model and grid sources

[3] — Gerber, J. M.; Magg, E.; Plez, B.; Bergemann, M.; Heiter, U.; Olander, T.; Hoppe, R. (2023). Non-LTE radiative transfer with Turbospectrum. A&A 669, A43 DOI: 10.1051/0004-6361/202243673. source record

[7] — Amarsi, A. M.; Lind, K.; Osorio, Y.; Nordlander, T.; Bergemann, M.; et al. (2020). The GALAH Survey: non-LTE departure coefficients for large spectroscopic surveys. A&A 642, A62 DOI: 10.1051/0004-6361/202038650. source record